Rendiconti Lincei. Scienze Fisiche e Naturali (2025) 36:1235–1248
https://doi.org/10.1007/s12210-025-01372-y

RESEARCH

Abundant new analytical wave solutions to the Schrödinger equations in optics via the double-variable expansion method

Md Mamunur Rasid[1] · Md Nur Hossain[2] · O. H. Khalil[3] · K. El-Rashidy[4] · Wen-Xiu Ma[5,6] · Md Mamun Miah[7,8]

Received: 13 June 2025 / Accepted: 27 September 2025 / Published online: 28 October 2025

Abstract

This study derives exact analytical solutions for three forms of the nonlinear Schrödinger equation (NLSE) with multiplicative noise in the Itô sense, using the double-variable expansion method. The selected models include a focusing-type NLSE (NLS^+), a defocusing-type NLSE (NLS^-), and a complex cubic NLSE with a delta potential. Through an appropriate wave transformation, the stochastic partial differential equations are reduced to nonlinear ordinary differential equations, enabling systematic application of the expansion method. The framework, constructed via auxiliary functions from a second-order linear ordinary differential equation, facilitates closed-form traveling wave solutions. These include solitonic, periodic, hyperbolic, and rational/rogue-wave-type structures. The method demonstrates robustness in addressing the effects of dispersion, nonlinearity, localized interactions, and stochastic perturbations in a unified analytical framework. Graphical illustrations highlight the dynamic behavior of these solutions under various parameter regimes, including wave number, stochastic noise intensity, and spectral parameters. The derived expressions serve as valuable benchmarks for validating numerical solvers and understanding the modulation and stability of nonlinear wave structures under noise, with potential applications in fiber optics, quantum information, and photonic device modeling. The novelty of this work is the extension of deterministic expansion techniques to stochastic systems, which provides closed-form solutions that accurately capture noise-modulated dynamics. Unlike conventional approaches, such as the inverse scattering transform and Darboux, Bäcklund transformations, the proposed framework accommodates a broader class of nonlinear models and captures richer waveforms. These results reinforce both the theoretical significance and physical relevance of the method, offering practical benchmarks for advancing nonlinear wave research in noisy environments.

✉ Md Nur Hossain
nur@ru.ac.bd

✉ O. H. Khalil
o.khalil@mu.edu.sa

✉ Wen-Xiu Ma
mawx@cas.usf.edu

✉ Md Mamun Miah
mamun0954@stu.kanazawa-u.ac.jp

[1] Faculty of Natural Sciences, Asian University for Women, 20/A, M. M, Mohammed Ali Rd, Chittagong 4000, Bangladesh

[2] Department of Mathematics, University of Rajshahi, Rajshahi 6205, Bangladesh

[3] Department of Mathematics, College of Science, Majmaah University, Al Majmaah 11952, Saudi Arabia

[4] Department of Mathematics, Faculty of Science, Beni-Suef University, Beni Suef 2722165, Egypt

[5] Department of Mathematics, Zhejiang Normal University, Jinhua 321004, Zhejiang, People's Republic of China

[6] Department of Mathematics and Statistics, University of South Florida, Tampa, FL 33620-5700, USA

[7] Division of Mathematical and Physical Sciences, Kanazawa University, Kakuma, Kanazawa 920-1192, Japan

[8] Department of Applied Mathematics, University of Rajshahi, Rajshahi 6205, Bangladesh

Graphic abstract

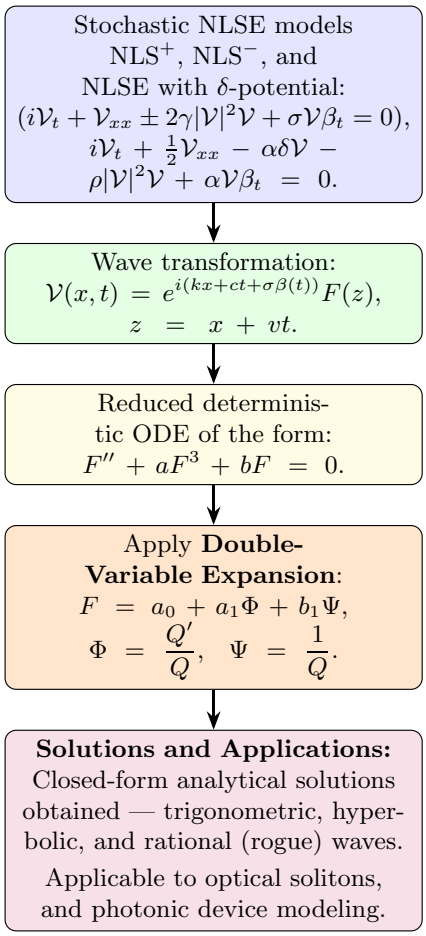

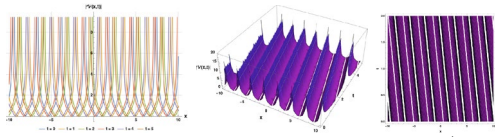

(a) Trigonometric solution for NLS^+

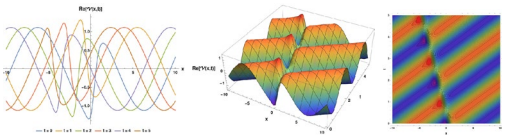

(b) Hyperbolic solution for NLS^-

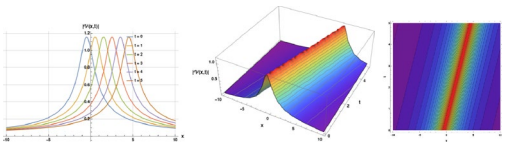

(c) Rational solution for $NLSE$ with δ-potential.

Analytical optical soliton solutions for stochastic NLSE models obtained via the double-variable expansion method, illustrating trigonometric, hyperbolic, and rational wave structures.

Keywords Nonlinear Schrödinger equation (NLSE) · Stochastic wave equations · Multiplicative noise · Soliton dynamics · Rogue wave structures · Analytical methods in optics

1 Introduction

Partial differential equations (PDEs) are essential tools for modeling diverse physical, biological, and engineering phenomena involving continuous change. From modeling fluid dynamics and heat conduction to predicting electromagnetic wave propagation and quantum behavior, PDEs form the backbone of theoretical modeling across the sciences. Nonlinear PDEs are especially important for capturing complex behaviors such as turbulence, soliton formation, pattern development, and chaos, which cannot be described using linear models (Hossain et al. 2024; Zafar et al. 2020; Akbar et al. 2021; Ashraf and Batool 2024; Hossain et al. 2024).

The nonlinear Schrödinger equation (NLSE) is a foundational pillar in the modeling of nonlinear wave propagation, arising in various fields, such as quantum mechanics, nonlinear optics, plasma physics, and Bose–Einstein condensation. It governs how wave packets evolve under the simultaneous influence of dispersion and nonlinearity, enabling the description of critical physical phenomena, such as solitons, modulational instability, and wave packet collapse. The significance of this equation goes far beyond pure mathematics, finding vital roles in the design and optimization of laser systems, fiber optics, and waveguides (Mirzazadeh et al. 2023; Alraddadi et al. 2024). With the increasing complexity of real-world systems, there is a growing need to account for environmental randomness and fluctuations. This has led to the emergence of the stochastic nonlinear Schrödinger equation (SNLSE), which incorporates random perturbations typically modeled as multiplicative white noise within the Itô calculus framework. The inclusion of stochastic effects is especially relevant in optical fibers, quantum communication channels,

and nanoscale devices, where noise influences both the shape and stability of waveforms (Alkhidhr 2023; Rehman et al. 2023; Shakeel et al. 2025). Exact solutions to these stochastic PDEs are valuable for both theoretical advances and practical applications. Such solutions can help explain the propagation of pulses in noisy environments, validate numerical simulations, and provide benchmark results for future theoretical models. However, solving nonlinear and stochastic PDEs analytically poses a significant challenge due to the coupling between nonlinearity and randomness. To address the analytical complexity of such nonlinear stochastic systems, a wide range of solution techniques have been developed, inverse scattering transform (Newell 1980), Darboux transformation (Li et al. 2021), Bäcklund transformation (Mimura 1978), GERF and NEDA techniques (Younas et al. 2022), and Painlevé analysis (Rizvi et al. 2021). In addition, several expansion-based techniques have gained popularity for their algorithmic structure and broad applicability. These include the tanh-coth method (Wang et al. 2024), the Sardar subequation method (Hossain et al. 2024), the sine-cosine method (Paux et al. 2025), the new generalized (G'/G) expansion method (Hossain et al. 2025), the improved Sardar subequation method (Hossain et al. 2024; Younas et al. 2023), the auxiliary equation method (Păuna 2024), Hirota Bilinear Method(Younas et al. 2022; Ismael et al. 2023; Az-Zo'bi et al. 2024; Ali et al. 2023), the modified generalized Riccati equation mapping method (Hamad and Ali 2024), Jacobi elliptic expansion function method (Ahmed and Ali 2024), the generalized G'/G expansion method (Atas et al. 2023), and extended sinh-Gordon equation expansion method (Sulaiman et al. 2021; Younas et al. 2021), each relying on trial functions and nonlinear transformations to simplify the original PDE. The auxiliary equation method, in particular, reduces the problem to solving simpler ODEs (such as Bernoulli, Riccati, or elliptic equations), providing a structured path toward exact traveling wave or soliton solutions. These methods have been successfully applied to various deterministic and stochastic models, including Korteweg–de Vries (KdV), sine-Gordon, Burgers, and Schrödinger-type equations (Al-Essa and ur Rahman 2024; Ahmad and Aldwoah 2024; Al-Askar 2023; Butt et al. 2024). Despite their successes, the application of these methods to stochastic settings—especially those with multiplicative noise in the Itô sense—remains less developed, prompting the need for generalized frameworks like the double-variable expansion method.

Despite these advances, the application of existing deterministic methods to stochastic NLSEs, particularly those driven by multiplicative noise in the Itô sense, remains limited. Most classical expansion-based approaches generate only restricted families of solutions and are not able to capture the full interplay between dispersion, nonlinearity, localized defects, and random perturbations. The motivation for the present work is therefore fourfold. First, stochastic NLSEs play a central role in describing pulse propagation in noisy optical fibers, quantum communication channels, and nonlinear photonic systems, but their analytical treatment is still underdeveloped (Alkhidhr 2023; Shakeel et al. 2025). Second, traditional methods, such as the inverse scattering transform, Darboux and Bäcklund transformations, or expansion-based techniques (Newell 1980; Li et al. 2021; Wang et al. 2024; Păuna 2024), have been successful for deterministic cases but cannot systematically address noise-modulated dynamics. Third, there is a strong need for a unified framework capable of producing diverse solution families, including solitons, periodic waves, and rogue waves, which can also serve as benchmarks to validate numerical solvers (Hossain et al. 2024, 2025). Finally, the novelty of the double-variable function expansion method lies in introducing two auxiliary functions instead of one, thus significantly broadening the class of obtainable solutions and extending deterministic expansion methods to stochastic contexts (Rasid et al. 2023; Al-Askar 2025).

The double-variable expansion method introduces two independent variables into the solution ansatz, usually representing combinations of the traveling wave variable and an auxiliary function. This approach allows for the construction of broader solution families–including periodic, solitary, and kink-type waves—by effectively capturing the interaction of dispersion and nonlinearity in a noise-dominated environment. Unlike single-variable techniques, the double-variable expansion method accommodates more complex structures, making it ideal for studying wave behavior in higher-dimensional and stochastic settings (Rizvi et al. 2024; Hossain et al. 2024; Al-Askar 2025). In recent studies, the double-variable expansion method has proven effective in generating exact solutions for various stochastic systems, including generalized Schrödinger–Hirota, Sasa–Satsuma, and Ginzburg–Landau equations (Raza et al. 2024; Hossain et al. 2024; Al-Askar 2023; Butt et al. 2024). These applications highlight its utility in capturing the evolution of bright, dark, breather, and dromion solutions even under the influence of multiplicative white noise. Moreover, the method provides a systematic framework that can be adapted to both deterministic and stochastic nonlinear equations, bridging a critical gap in current analytical methodologies.

In this paper, we apply the double-variable expansion method to obtain novel closed-form solutions for a class of stochastic Schrödinger equations driven by multiplicative noise. Our aim is to explore how noise intensity, dispersion parameters, and nonlinear coefficients affect the resulting wave profiles. The solutions we obtained are expected to contribute to a better understanding of pulse dynamics in noisy optical media and potentially inform the design of

resilient optical systems and quantum information networks. The solutions derived herein also possess theoretical value in mathematical physics, where they can be used to test the accuracy of numerical solvers, explore stability regimes, and benchmark various noise-influenced dynamics. Furthermore, these analytical expressions offer visual and intuitive insight into how solitons and other nonlinear structures are modulated by stochastic perturbations in real time.

The paper is structured to systematically develop and apply the double-variable expansion method to a class of stochastic nonlinear Schrödinger equations. Section 2 introduces the specific form of the stochastic Schrödinger equation considered in this work, incorporating multiplicative noise in the Itô sense and formulating it in a way suitable for analytical solution techniques. Section 3 provides a comprehensive overview of the double-variable expansion method, detailing the necessary transformations, assumptions, and the structure of the trial function. In Sect. 4, we apply the expansion framework to derive exact solutions of the equation, supported by graphical illustrations that showcase the waveforms for various parameter regimes. Section 5 discusses the physical significance of the obtained solutions, with an emphasis on their behavior under stochastic perturbations, stability considerations, and implications for applications in nonlinear optical systems. Finally, Sect. 6 summarizes the key findings, highlights the strengths and limitations of the employed method, and suggests avenues for future research in related stochastic nonlinear systems.

2 Model equation

For the sake of simplicity, let us consider the three models of the nonlinear Schrödinger equations driven by multiplicative noise in the Itô sense as NLSEI. Initially, our focus is on the NLSEI presented in Bhrawy et al. (2014), which is denoted as NLS^{+}. The NLS^{+} is given in Bhrawy et al. (2014) is as follows:

$$i\mathcal{V}_t + \mathcal{V}_{xx} + 2\gamma\,|\mathcal{V}|^2\mathcal{V} + \sigma\mathcal{V}\beta_t = 0. \tag{2.1}$$

Next, we have considered the NLSE labeled as NLS^{-} which can be written as follows:

$$i\mathcal{V}_t + \mathcal{V}_{xx} - 2\gamma\,|\mathcal{V}|^2\mathcal{V} + \sigma\mathcal{V}\beta_t = 0. \tag{2.2}$$

Here, $\gamma \in \mathbb{R} - \{0\}$ represents the nonlinear coefficient $\mathcal{V}(x,t)$ is a complex-valued function. The parameter σ characterizes the intensity of the stochastic perturbation. The term $\mathcal{V}_{xx}$ accounts for dissipative effects, while the nonlinear interaction is captured by $\|\mathcal{V}\|^2\mathcal{V}$. The noise component β_t corresponds to the temporal derivative of the Brownian motion $\beta(t)$.

We finally considered the NLSE forced by multiplicative noise in the Ito sense labeled as the Complex Cubic NLSE with δ-potential and given by Baskonus et al. (2018)

$$i\mathcal{V}_t + \frac{1}{2}\mathcal{V}_{xx} - \alpha\delta\mathcal{V} - \rho|\mathcal{V}|^2\mathcal{V} + \alpha\mathcal{V}\beta_t = 0. \tag{2.3}$$

In this formulation, the parameters β, δ, and ρ belong to the set $\mathbb{R} - \{0\}$, where δ denotes the Dirac delta function centered at the origin. The delta interaction is termed *attractive* when $\alpha < 0$, and *repulsive* when $\alpha > 0$ [44]. The stability of solutions to Eq. (1.3) was examined in Goodman et al. (2004), while the dynamics of the associated flow were explored in Holmer and Zworski (2007). A solution to the same model using the variational approach was provided in Fukuizumi et al. (2008). Notably, these studies considered the system without the influence of stochastic perturbations.

3 The double-variable function (Φ, Ψ) expansion process

Let us consider the double-variable function (Φ, Ψ) for the following second-order linear ordinary differential equation (Hossain et al. 2024; Rasid et al. 2023):

$$\mathrm{Q}''(z) + \lambda \mathrm{Q}(z) = \mu, \tag{3.1}$$

where

$$\Phi := \frac{\mathrm{Q}'(z)}{\mathrm{Q}(z)}, \Psi := \frac{1}{\mathrm{Q}(z)}. \tag{3.2}$$

Then, we can obtain

$$\Phi' = -\Phi^2 + \mu\Psi - \lambda \text{ and } \Psi' = -\Phi\Psi, \tag{3.3}$$

where Φ' and Ψ' represent the first derivative Φ and Ψ respect to z. The solutions of Eq. 3.1 can be divided into three non-intersecting cases for three different possible real values of r as follows:

Instance 1: If the value of λ is positive, then all possible exact analytical solutions (EAS) of Eq. 3.1 are given by

$$Q(z) = \mathcal{A}_1 \sin\left(z\sqrt{\lambda}\right) + \mathcal{A}_2 \cos\left(z\sqrt{\lambda}\right) + \frac{\mu}{\lambda}, \tag{3.4}$$

with the condition

$$\Psi^2 = \frac{\lambda\left(\Phi^2 - 2\mu\Psi + \lambda\right)}{\lambda^2\delta_1 - \mu^2} \tag{3.5}$$

and $\delta_1 = {\mathcal{A}_1}^2 + {\mathcal{A}_2}^2$.

Instance 2: On the contrary, if $\lambda < 0$, then EASs of Eq. 3.1 are

$$Q(z) = \mathcal{A}_1 \sinh\left(z\sqrt{-\lambda}\right) + \mathcal{A}_2 \cosh\left(z\sqrt{-\lambda}\right) + \frac{\mu}{\lambda}, \quad (3.6)$$

where

$$\Psi^2 = \frac{-\lambda\left(\Phi^2 - 2\mu\Psi + \lambda\right)}{\lambda^2\delta_2 + \mu^2} \quad (3.7)$$

and $\delta_2 = {\mathcal{A}_1}^2 - {\mathcal{A}_2}^2$.

Instance 3: Finally, for the zero value of λ, Eq. 3.1 provides the following EASs:

$$Q(z) = \frac{\mu}{2}z^2 + \mathcal{A}_1 z + \mathcal{A}_2, \quad (3.8)$$

with

$$\Psi^2 = \frac{\left(\Phi^2 - 2\mu\Psi\right)}{{\mathcal{A}_1}^2 - 2\mu\mathcal{A}_2}. \quad (3.9)$$

4 NLPDE to PDE

Let us consider the NLPDE as

$$\mathcal{R}(\mathcal{V}, \mathcal{V}_x, \mathcal{V}_t, \mathcal{V}_{xx}, \mathcal{V}_{tt}, \mathcal{V}_{tx}, ...) = 0, \quad (4.1)$$

where $\mathcal{R}$ is a polynomial in $\mathcal{V}$ and its partial derivatives. Consider the following wave transformation:

$$\mathcal{V}(x,t) = \mathcal{V}(z),\ z = x + \nu t, \quad (4.2)$$

where ρ is the wave velocity. Now, using Eq. 4.2 in Eq. 4.1, we have the following ordinary differential equation:

$$\mathcal{H}(\mathcal{V}, \mathcal{V}', \nu\mathcal{V}', \mathcal{V}'', \nu^2\mathcal{V}'', \nu\mathcal{V}'', ...) = 0. \quad (4.3)$$

Finally, let us consider that solution of Eq. 4.3 by double-variable function expansion methods is given by

$$\mathcal{V}(z) = a_0 + \sum_{i=1}^{K} a_i \Phi^i(z) + \sum_{i=1}^{K} b_i \Phi^{i-1}(z)\Psi^i(z). \quad (4.4)$$

In this context, Φ and Ψ are defined as in Eq. 3.2, and the parameters a_0, a_i, b_i for $i = 1, 2, 3, \ldots, K$ are treated as arbitrary constants. The value of the balance number K is determined through the application of the homogeneous balance method, leading to the explicit form of the solution presented in Eq. 4.4.

Substituting Eq. 4.4 into Eq. 4.3, and analyzing each of the three distinct cases previously outlined, the left-hand side of Eq. 4.3 transforms into a polynomial in Φ and Ψ, with coefficients expressed in terms of the arbitrary constants. Importantly, the degree of Φ in this polynomial remains less than or equal to one.

By setting the coefficients of all distinct monomial terms to zero, a system of algebraic equations involving the constants a_0, a_1, b_1, ρ, and b_1 is obtained. This nonlinear system is solved using symbolic computation (Mathematica), yielding specific parameter values. Substituting these values back into Eqs. 3.2, 4.2, and 4.4 yields the exact analytical solutions corresponding to each of the three considered scenarios.

5 Analytical framework for constructing exact solutions of the Schrödinger equation

To derive closed-form solutions for the three stochastic nonlinear Schrödinger equations (NLSEs) considered in this study, we employ a systematic reduction procedure based on the double-variable function expansion method. This framework allows for the analytical handling of nonlinearities and stochastic influences present in the equations.

5.1 Reduction via wave transformation

We begin by applying a wave transformation to convert each nonlinear partial differential equation (PDE) into a corresponding ordinary differential equation (ODE). The transformation is given by

$$V(x,t) = e^{i(kx+ct+\sigma\beta(t))}F(z), \quad z = x + \nu t, \quad (5.1)$$

where p, r, and v are constants associated with wave number, frequency, and velocity, respectively, and $\beta(t)$ denotes standard Brownian motion, modeling the stochastic perturbations in the Itô sense.

Substituting this transformation into each governing equation of NLS$^+$ and NLS$^-$ yields the following reduced forms:

For the NLS$^+$ model:

$$F''(z) + 2\gamma F^3(z) - (k^2 + c)F(z) = 0, \quad v = -2k. \quad (5.2)$$

For the NLS$^-$ model:

$$F''(z) - 2\gamma F^3(z) - (k^2 + c)F(z) = 0, \quad v = -2k. \quad (5.3)$$

For the NLSE with delta potential, the transformation is used

$$V(x,t) = e^{i(kx+ct+k+\sigma\beta(t))}F(z), \quad z = \eta(x - \nu t), \quad (5.4)$$

$$\eta^2 F''(z) - 2\rho F^3(z) - (k^2 + 2(c + \alpha\delta))F(z) = 0, \quad v = k, \quad (5.5)$$

where η, ρ, α, and δ are additional parameters arising from delta-type interactions and noise strength.

5.2 Construction of the trial solution

Next, we determine the structure of the solution using the homogeneous balance principle. Balancing the highest-order nonlinear and derivative terms reveals a balance number $K = 1$. Hence, we propose the solution in the form

$$F(z) = a_0 + a_1\Phi(z) + b_1\Psi(z), \tag{5.6}$$

where $\Phi(z)$ and $\Psi(z)$ are auxiliary functions defined as

$$\Phi = \frac{Q'}{Q}, \quad \Psi = \frac{1}{Q}, \tag{5.7}$$

and $Q(z)$ satisfies the linear second-order ODE

$$Q''(z) + \lambda Q(z) = \mu. \tag{5.8}$$

5.3 Solution strategy

Substituting the proposed solution into the reduced ODE yields a polynomial in Φ and Ψ, where each term is a function of the unknown constants. To determine these constants (a_0, a_1, b_1, λ, μ, etc.), we set the coefficients of each distinct monomial to zero, resulting in a nonlinear system of algebraic equations (Hossain et al. 2024; Cinar et al. 2022).

This system is solved using symbolic computation software such as *Mathematica*, allowing us to find consistent parameter sets under three distinct scenarios based on the sign of λ:

Case I ($\lambda > 0$): leads to trigonometric solutions,

Case II ($\lambda < 0$): produces hyperbolic function-based solutions,

Case II ($\lambda = 0$): yields rational function solutions.

These analytical expressions provide a wide variety of wave profiles, including periodic, solitary, and rational structures. The derived solutions are presented in detail in the following subsections and interpreted in terms of their physical significance for optical systems under stochastic effects.

6 Analytical solutions for the three NLSE models

6.1 Solutions to the NLS$^+$ model

Having developed the necessary analytical framework using the double-variable expansion method, we now initiate its application to the first model under consideration—the nonlinear Schrödinger equation with a focusing-type nonlinearity, denoted as NLS^+. This equation serves as a fundamental benchmark for investigating the interplay between dispersion and positive cubic nonlinearity under stochastic influences. Through the previously introduced wave transformation, the stochastic partial differential equation is reduced to a nonlinear ordinary differential equation. We proceed to analyze this equation by constructing closed-form solutions categorized according to three distinct cases of the spectral parameter λ: positive, negative, and zero. Each case reveals unique structural features in the wave profile, enabling us to characterize diverse solution behaviors, including oscillatory, localized, and rational-type waveforms.

Case I ($\lambda > 0$): The values of the variables are $a_0 = 0$, $a_1 = \pm\frac{i}{2\sqrt{\gamma}}$, $b_1 = \pm\frac{\sqrt{\mu^2-\lambda^2\delta_1}}{2\sqrt{\gamma}\sqrt{\lambda}}$, and $c = \frac{1}{2}(\lambda - 2k^2)$.

Therefore

$$\mathcal{F}(z) = \pm\frac{i}{2\sqrt{\gamma}}\frac{\mathcal{A}_1\sqrt{\lambda}\cos(z\sqrt{\lambda}) - \mathcal{A}_2\sqrt{\lambda}\sin(z\sqrt{\lambda})}{\mathcal{A}_1\sin(z\sqrt{\lambda}) + \mathcal{A}_2\cos(z\sqrt{\lambda}) + \frac{\mu}{\lambda}} \pm \frac{\sqrt{\mu^2-\lambda^2\delta_1}}{2\sqrt{\gamma}\sqrt{\lambda}} \cdot \frac{1}{\mathcal{A}_1\sin(z\sqrt{\lambda}) + \mathcal{A}_2\cos(z\sqrt{\lambda}) + \frac{\mu}{\lambda}}$$

and

$$\mathcal{V}(x,t) = e^{i(kx+ct+\sigma\beta(t))} \left(\pm\frac{i}{2\sqrt{\gamma}}\frac{\mathcal{A}_1\sqrt{\lambda}\cos(z\sqrt{\lambda}) - \mathcal{A}_2\sqrt{\lambda}\sin(z\sqrt{\lambda})}{\mathcal{A}_1\sin(z\sqrt{\lambda}) + \mathcal{A}_2\cos(z\sqrt{\lambda}) + \frac{\mu}{\lambda}} = e^{i(kx+ct+\sigma b_1(t))} \pm \frac{\sqrt{\mu^2-\lambda^2\delta_1}}{2\sqrt{\gamma}\sqrt{\lambda}} \cdot \frac{1}{\mathcal{A}_1\sin(z\sqrt{\lambda}) + \mathcal{A}_2\cos(z\sqrt{\lambda}) + \frac{\mu}{\lambda}}\right), \quad z = x + vt. \tag{6.1}$$

Case II ($\lambda < 0$):

The values of the variables are

$$a_0 = 0,\ a_1 = \pm\frac{i}{2\sqrt{\gamma}}, \quad b_1 = \pm\frac{\sqrt{\delta_2\lambda^2+\mu^2}}{2\sqrt{\gamma}\sqrt{\lambda}}, \quad c = \frac{1}{2}(\lambda - 2k^2).$$

Therefore

$$\mathcal{F}(z) = \pm\frac{i}{2\sqrt{\gamma}} \cdot \frac{\mathcal{A}_1\sqrt{-\lambda}\cosh(z\sqrt{-\lambda}) + \mathcal{A}_2\sqrt{-\lambda}\sinh(z\sqrt{-\lambda})}{\mathcal{A}_1\sinh(z\sqrt{-\lambda}) + \mathcal{A}_2\cosh(z\sqrt{-\lambda}) + \frac{\mu}{\lambda}} \pm \frac{\sqrt{\delta_2\lambda^2+\mu^2}}{2\sqrt{\gamma}\sqrt{\lambda}} \cdot \frac{1}{\mathcal{A}_1\sinh(z\sqrt{-\lambda}) + \mathcal{A}_2\cosh(z\sqrt{-\lambda}) + \frac{\mu}{\lambda}}$$

and

$$\mathcal{V}(x,t) = e^{i(kx+ct+\sigma\beta(t))}$$
$$\left(\pm\frac{i}{2\sqrt{\gamma}}\cdot\frac{\mathcal{A}_1\sqrt{-\lambda}\cosh(z\sqrt{-\lambda})+\mathcal{A}_2\sqrt{-\lambda}\sinh(z\sqrt{-\lambda})}{\mathcal{A}_1\sinh(z\sqrt{-\lambda})+\mathcal{A}_2\cosh(z\sqrt{-\lambda})+\frac{\mu}{\lambda}}\right.$$
$$= e^{i(kx+ct+\sigma\beta(t))}\pm\frac{\sqrt{\delta_2\lambda^2+\mu^2}}{2\sqrt{\gamma}\sqrt{\lambda}} \tag{6.2}$$
$$\left.\cdot\frac{1}{\mathcal{A}_1\sinh(z\sqrt{-\lambda})+\mathcal{A}_2\cosh(z\sqrt{-\lambda})+\frac{\mu}{\lambda}}\right),\quad z=x+vt.$$

Case III ($\lambda = 0$): The values of the variables are

$$a_1 = \pm\frac{i}{2\sqrt{\gamma}},\quad b_1 = \pm\frac{\sqrt{-\mathcal{A}_1^2+2\mu\mathcal{A}_2}}{2\sqrt{\gamma}},\quad c=-k^2,\quad z=x+vt.$$

Therefore

$$\mathcal{F}(z) = \pm\frac{i}{2\sqrt{\gamma}}\cdot\frac{\mu z+\mathcal{A}_1}{\frac{\mu}{2}z^2+\mathcal{A}_1 z+\mathcal{A}_2} \pm\frac{\sqrt{-\mathcal{A}_1^2+2\mu\mathcal{A}_2}}{2\sqrt{\gamma}}\cdot\frac{1}{\frac{\mu}{2}z^2+\mathcal{A}_1 z+\mathcal{A}_2}$$

and

$$\mathcal{V}(x,t) = e^{i(kx+ct+\sigma\beta(t))}\left(\pm\frac{i}{2\sqrt{\gamma}}\cdot\frac{\mu z+\mathcal{A}_1}{\frac{\mu}{2}z^2+\mathcal{A}_1 z+\mathcal{A}_2 = e^{i(kx+ct+\sigma b_1(t))}}\right.$$
$$\left.\pm\frac{\sqrt{-\mathcal{A}_1^2+2\mu\mathcal{A}_2}}{2\sqrt{\gamma}}\cdot\frac{1}{\frac{\mu}{2}z^2+\mathcal{A}_1 z+\mathcal{A}_2}\right),\quad z=x+vt. \tag{6.3}$$

6.2 Solutions to the NLS$^-$ model

Having established the closed-form solutions for the *NLS*$^+$ model under three distinct cases of the spectral parameter λ, we now extend our analysis to its complementary form—the *NLS*$^-$ model. Although structurally similar, the *NLS*$^-$ equation introduces a crucial sign change in the nonlinear term, which leads to distinct solution behavior and physical interpretations.

Case I ($\lambda > 0$):

The values of the variables are

$$a_0 = 0,\ a_1 = \pm\frac{1}{2\sqrt{\gamma}},\quad b_1 = \pm\frac{\sqrt{\lambda^2\delta_1-\mu^2}}{2\sqrt{\gamma}\sqrt{\lambda}},\quad c=\frac{1}{2}(\lambda-2k^2).$$

Therefore

$$\mathcal{F}(z) = \pm\frac{1}{2\sqrt{\gamma}}\cdot\frac{\mathcal{A}_1\sqrt{\lambda}\cos(z\sqrt{\lambda})-\mathcal{A}_2\sqrt{\lambda}\sin(z\sqrt{\lambda})}{\mathcal{A}_1\sin(z\sqrt{\lambda})+\mathcal{A}_2\cos(z\sqrt{\lambda})+\frac{\mu}{\lambda}} \pm\frac{\sqrt{\lambda^2\delta_1-\mu^2}}{2\sqrt{\gamma}\sqrt{\lambda}}\cdot\frac{1}{\mathcal{A}_1\sin(z\sqrt{\lambda})+\mathcal{A}_2\cos(z\sqrt{\lambda})+\frac{\mu}{\lambda}}.$$

Therefore

$$\mathcal{V}(x,t) = e^{i(kx+ct+\sigma\beta(t))}$$
$$\left(\pm\frac{1}{2\sqrt{\gamma}}\cdot\frac{\mathcal{A}_1\sqrt{\lambda}\cos(z\sqrt{\lambda})-\mathcal{A}_2\sqrt{\lambda}\sin(z\sqrt{\lambda})}{\mathcal{A}_1\sin(z\sqrt{\lambda})+\mathcal{A}_2\cos(z\sqrt{\lambda})+\frac{\mu}{\lambda}}\right.$$
$$= e^{i(kx+ct+\sigma\beta(t))}\pm\frac{\sqrt{\lambda^2\delta_1-\mu^2}}{2\sqrt{\gamma}\sqrt{\lambda}} \tag{6.4}$$
$$\left.\cdot\frac{1}{\mathcal{A}_1\sin(z\sqrt{\lambda})+\mathcal{A}_2\cos(z\sqrt{\lambda})+\frac{\mu}{\lambda}}\right),\quad z=x+vt.$$

Case II ($\lambda < 0$):

The values of the variables are

$$a_1 = \pm\frac{1}{2\sqrt{\gamma}},\quad b_1 = \pm\frac{\sqrt{-\delta_2\lambda^2-\mu^2}}{2\sqrt{\gamma}\sqrt{\lambda}},\quad c=\frac{1}{2}(\lambda-2k^2).$$

Therefore

$$\mathcal{F}(z) = \pm\frac{1}{2\sqrt{\gamma}}\cdot\frac{\mathcal{A}_1\sqrt{-\lambda}\cosh(z\sqrt{-\lambda})+\mathcal{A}_2\sqrt{-\lambda}\sinh(z\sqrt{-\lambda})}{\mathcal{A}_1\sinh(z\sqrt{-\lambda})+\mathcal{A}_2\cosh(z\sqrt{-\lambda})+\frac{\mu}{\lambda}} \pm\frac{\sqrt{-\delta_2\lambda^2-\mu^2}}{2\sqrt{\gamma}\sqrt{\lambda}}\cdot\frac{1}{\mathcal{A}_1\sinh(z\sqrt{-\lambda})+\mathcal{A}_2\cosh(z\sqrt{-\lambda})+\frac{\mu}{\lambda}}$$

and

$$\mathcal{V}(x,t) = e^{i(kx+ct+\sigma\beta(t))}$$
$$\left(\pm\frac{1}{2\sqrt{\gamma}}\cdot\frac{\mathcal{A}_1\sqrt{-\lambda}\cosh(z\sqrt{-\lambda})+\mathcal{A}_2\sqrt{-\lambda}\sinh(z\sqrt{-\lambda})}{\mathcal{A}_1\sinh(z\sqrt{-\lambda})+\mathcal{A}_2\cosh(z\sqrt{-\lambda})+\frac{\mu}{\lambda}=e^{i(kx+ct+\sigma\beta(t))}}\right.$$
$$\left.\pm\frac{\sqrt{-\delta_2\lambda^2-\mu^2}}{2\sqrt{\gamma}\sqrt{\lambda}}\cdot\frac{1}{\mathcal{A}_1\sinh(z\sqrt{-\lambda})+\mathcal{A}_2\cosh(z\sqrt{-\lambda})+\frac{\mu}{\lambda}}\right),\quad z=x+vt. \tag{6.5}$$

Case III ($\lambda = 0$):

$$a_1 = \pm\frac{1}{2\sqrt{\gamma}},\quad b_1 = \pm\frac{\sqrt{\mathcal{A}_1^2-2\mathcal{A}_2\mu}}{2\sqrt{\gamma}},\quad c=-k^2,$$

$$\mathcal{F}(z) = \pm\frac{1}{2\sqrt{\gamma}}\cdot\frac{\mu z+\mathcal{A}_1}{\frac{\mu}{2}z^2+\mathcal{A}_1 z+\mathcal{A}_2}\pm\frac{\sqrt{\mathcal{A}_1^2-2\mathcal{A}_2\mu}}{2\sqrt{\gamma}}\cdot\frac{1}{\frac{\mu}{2}z^2+\mathcal{A}_1 z+\mathcal{A}_2}$$

and

$$\mathcal{V}(x,t) = e^{i(kx+ct+\sigma\beta(t))}\left(\pm\frac{1}{2\sqrt{\gamma}}\cdot\frac{\mu z+\mathcal{A}_1}{\frac{\mu}{2}z^2+\mathcal{A}_1 z+\mathcal{A}_2} \pm\frac{\sqrt{\mathcal{A}_1^2-2\mathcal{A}_2\mu}}{2\sqrt{\gamma}}\cdot\frac{1}{\frac{\mu}{2}z^2+\mathcal{A}_1 z+\mathcal{A}_2}\right),\quad z=x+vt. \tag{6.6}$$

6.3 Solutions to the NLSE with delta potential

Following the solution procedure for the NLS^{-} equation, we turn our attention to a more complex configuration: the stochastic nonlinear Schrödinger equation with a delta potential. This model introduces a localized interaction at the origin via the Dirac delta function and poses new analytical challenges. Nonetheless, the double-variable expansion framework remains effective for generating exact solutions in this setting.

Case I ($\lambda > 0$):

$$a_0 = 0,\ a_1 = \pm\frac{\eta}{2\sqrt{\rho}},\quad b_1 = \pm\frac{\sqrt{\delta_1\eta^2\lambda^2-\eta^2\mu^2}}{2\sqrt{\lambda}\sqrt{\rho}},$$
$$c = \frac{1}{4}\left(-4\alpha\delta+\eta^2\lambda-2k^2\right).$$

Therefore

$$\mathcal{F}(z) = \pm\frac{\eta}{2\sqrt{\rho}}\cdot\frac{\mathcal{A}_1\sqrt{\lambda}\cos(z\sqrt{\lambda})-\mathcal{A}_2\sqrt{\lambda}\sin(z\sqrt{\lambda})}{\mathcal{A}_1\sin(z\sqrt{\lambda})+\mathcal{A}_2\cos(z\sqrt{\lambda})+\frac{\mu}{\lambda}} \pm\frac{\sqrt{\delta_1\eta^2\lambda^2-\eta^2\mu^2}}{2\sqrt{\lambda}\sqrt{\rho}}\cdot\frac{1}{\mathcal{A}_1\sin(z\sqrt{\lambda})+\mathcal{A}_2\cos(z\sqrt{\lambda})+\frac{\mu}{\lambda}}$$

and

$$\mathcal{V}(x,t) = e^{i(kx+ct+k+\sigma\beta(t))}\left(\pm\frac{\eta}{2\sqrt{\rho}}\cdot\frac{\mathcal{A}_1\sqrt{\lambda}\cos(z\sqrt{\lambda})-\mathcal{A}_2\sqrt{\lambda}\sin(z\sqrt{\lambda})}{\mathcal{A}_1\sin(z\sqrt{\lambda})+\mathcal{A}_2\cos(z\sqrt{\lambda})+\frac{\mu}{\lambda}} = e^{i(kx+ct+\sigma b_1(t))}\pm\frac{\sqrt{\delta_1\eta^2\lambda^2-\eta^2\mu^2}}{2\sqrt{\lambda}\sqrt{\rho}}\cdot\frac{1}{\mathcal{A}_1\sin(z\sqrt{\lambda})+\mathcal{A}_2\cos(z\sqrt{\lambda})+\frac{\mu}{\lambda}}\right),$$
$$z=\eta(x-vt),\ v=k. \tag{6.7}$$

Case II ($\lambda < 0$):

$$a_0 = 0,\ a_1 = \pm\frac{\eta}{2\sqrt{\rho}},\quad b_1 = \pm\frac{i\eta\sqrt{\delta_2\lambda^2+\mu^2}}{2\sqrt{\lambda}\sqrt{\rho}},$$
$$c = \frac{1}{4}\left(-2k^2-4\alpha\delta+\eta^2\lambda\right).$$

Therefore

$$\mathcal{F}(z) = \pm\frac{\eta}{2\sqrt{\rho}}\cdot\frac{\mathcal{A}_1\sqrt{-\lambda}\cosh(z\sqrt{-\lambda})+\mathcal{A}_2\sqrt{-\lambda}\sinh(z\sqrt{-\lambda})}{\mathcal{A}_1\sinh(z\sqrt{-\lambda})+\mathcal{A}_2\cosh(z\sqrt{-\lambda})+\frac{\mu}{\lambda}} \pm\frac{i\eta\sqrt{\delta_2\lambda^2+\mu^2}}{2\sqrt{\lambda}\sqrt{\rho}}\cdot\frac{1}{\mathcal{A}_1\sinh(z\sqrt{-\lambda})+\mathcal{A}_2\cosh(z\sqrt{-\lambda})+\frac{\mu}{\lambda}}$$

and

$$\mathcal{V}(x,t) = e^{i(kx+ct+k+\sigma\beta(t))}\left(\pm\frac{\eta}{2\sqrt{\rho}}\cdot\frac{\mathcal{A}_1\sqrt{-\lambda}\cosh(z\sqrt{-\lambda})+\mathcal{A}_2\sqrt{-\lambda}\sinh(z\sqrt{-\lambda})}{\mathcal{A}_1\sinh(z\sqrt{-\lambda})+\mathcal{A}_2\cosh(z\sqrt{-\lambda})+\frac{\mu}{\lambda}} = e^{i(kx+ct+\sigma b_1(t))}\pm\frac{i\eta\sqrt{\delta_2\lambda^2+\mu^2}}{2\sqrt{\lambda}\sqrt{\rho}}\cdot\frac{1}{\mathcal{A}_1\sinh(z\sqrt{-\lambda})+\mathcal{A}_2\cosh(z\sqrt{-\lambda})+\frac{\mu}{\lambda}}\right),$$
$$z=\eta(x-vt),\ v=k. \tag{6.8}$$

Case III ($\lambda = 0$):

$$a_0 = 0,\ a_1 = \pm\frac{\eta}{2\sqrt{\rho}},\quad b_1 = \pm\frac{\sqrt{\eta^2\mathcal{A}_1^2-2\eta^2\mu\mathcal{A}_2}}{2\sqrt{\rho}},$$
$$c = \frac{1}{2}\left(-k^2-2\alpha\delta\right).$$

Therefore

$$\mathcal{F}(z) = \pm\frac{\eta}{2\sqrt{\rho}}\cdot\frac{\mu z+\mathcal{A}_1}{\frac{\mu}{2}z^2+\mathcal{A}_1 z+\mathcal{A}_2} \pm\frac{\sqrt{\eta^2\mathcal{A}_1^2-2\eta^2\mu\mathcal{A}_2}}{2\sqrt{\rho}}\cdot\frac{1}{\frac{\mu}{2}z^2+\mathcal{A}_1 z+\mathcal{A}_2}$$

and

$$\mathcal{V}(x,t) = e^{i(kx+ct+k+\sigma\beta(t))}\left(\pm\frac{\eta}{2\sqrt{\rho}}\cdot\frac{\mu z+\mathcal{A}_1}{\frac{\mu}{2}z^2+\mathcal{A}_1 z+\mathcal{A}_2} = e^{i(kx+ct+\sigma b_1(t))}\pm\frac{\sqrt{\eta^2\mathcal{A}_1^2-2\eta^2\mu\mathcal{A}_2}}{2\sqrt{\rho}}\cdot\frac{1}{\frac{\mu}{2}z^2+\mathcal{A}_1 z+\mathcal{A}_2}\right),$$
$$z=\eta(x-vt),\ v=k. \tag{6.9}$$

7 Graphical interpretations of some solutions

In this section of the paper, we have plotted several analytical solutions of the stochastic nonlinear Schrödinger equation models using the double-variable function expansion method for selected parameter values. In the graphical representations, we have plotted the modulus $|\mathcal{V}(x,t)|$ of the solutions rather than the squared modulus

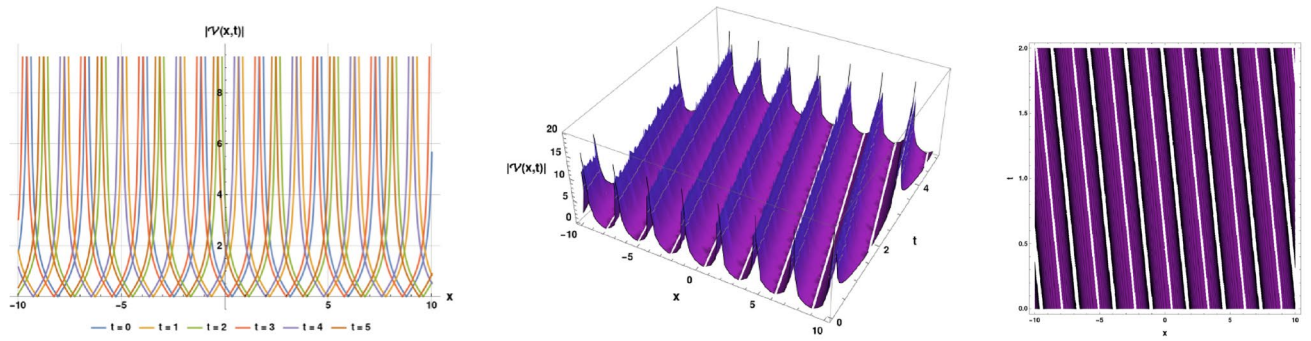

(a) 2D (b) 3D (c) Contour

Fig. 1 Graph of the solution $|\mathcal{V}(x,t)|$ corresponding to Eq. 6.1 for the following values of the constants, $k = \gamma = \mu = 1,\ \sigma = 0,\ \lambda = 5,\ \mathcal{A}_1 = -0.5,\ \mathcal{A}_2 = 0.75,\ \beta(t) = \sin(t)$ and $t = 0$ to 5

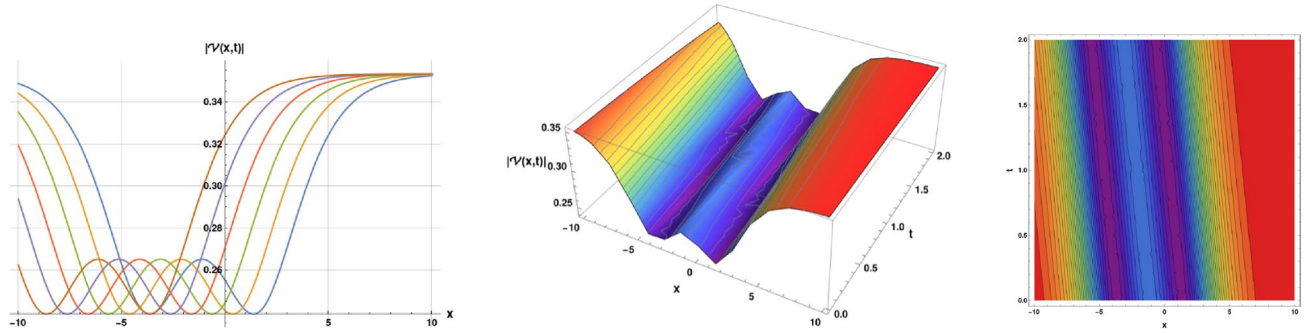

(a) 2D (b) 3D (c) Contour

Fig. 2 Graph of the solution $|\mathcal{V}(x,t)|$ corresponding to Eq. 6.2 for the following values of the constants, $k = \gamma = \mu = 1,\ \sigma = 0,\ \lambda = -0.5,\ \mathcal{A}_1 = -0.5,\ \mathcal{A}_2 = -0.75,\ \beta(t) = \sin(t)$ and $t = 0$ to 5

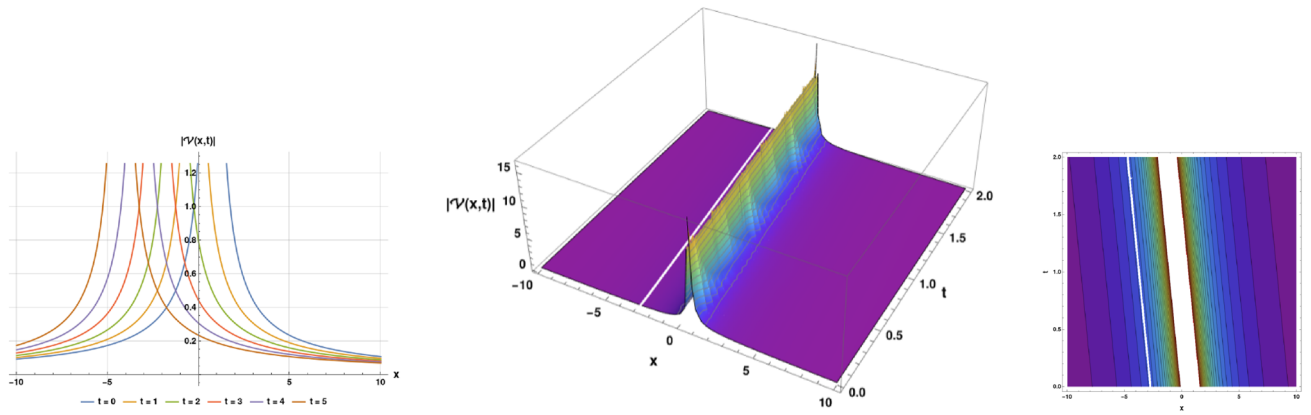

(a) 2D (b) 3D (c) Contour

Fig. 3 Graph of the solution $|\mathcal{V}(x,t)|$ corresponding to Eq. 6.3 for the following values of the constants, $k = \gamma = \mu = 1,\ \sigma = 0,\ \mathcal{A}_1 = 1,\ \mathcal{A}_2 = -1,\ \beta(t) = \sin(t)$ and $t = 0$ to 5

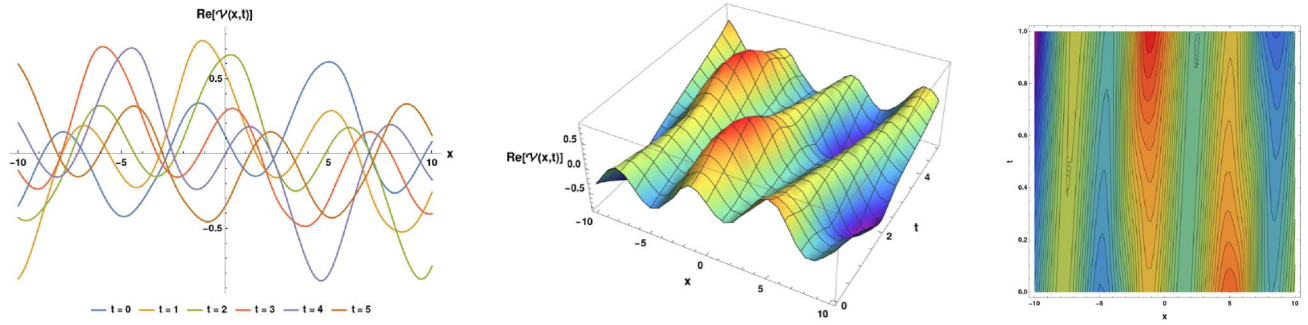

(a) 2D (b) 3D (c) Contour

Fig. 4 Graph of the real part of the solution $\mathcal{V}(x,t)$ corresponding to Eq. 6.4 for the following values of the constants, $k = \gamma = \mu = 1,\ \sigma = 0,\ \lambda = 0.5\ \mathcal{A}_1 = 1,\ \mathcal{A}_2 = 1,\ \beta(t) = sin(t)$ and $t = 0$ to 5

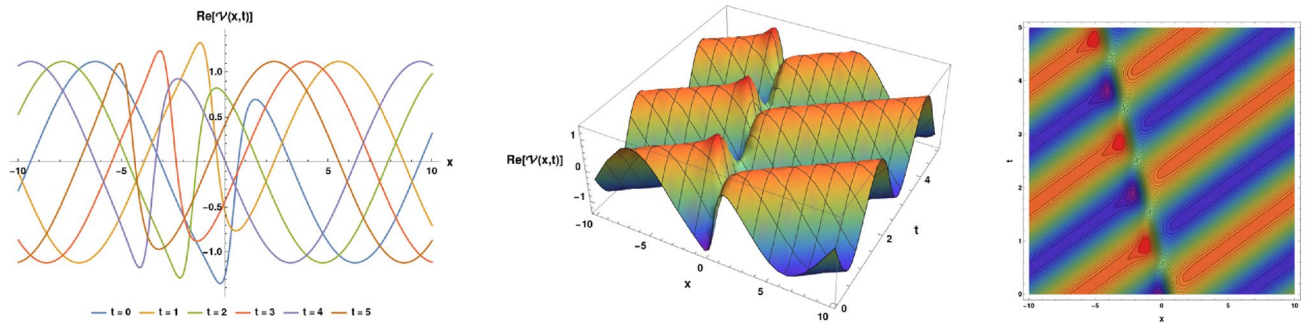

(a) 2D (b) 3D (c) Contour

Fig. 5 Graph of the real part of the solution $\mathcal{V}(x,t)$ corresponding to Eq. 6.5 for the following values of the constants, $k = 0.5, \gamma = \mu = 1,\ \sigma = 0,\ \lambda = -5,\ \mathcal{A}_1 = 0.5,\ \mathcal{A}_2 = -1,\ \beta(t) = \sin(t)$ and $t = 0$ to 5

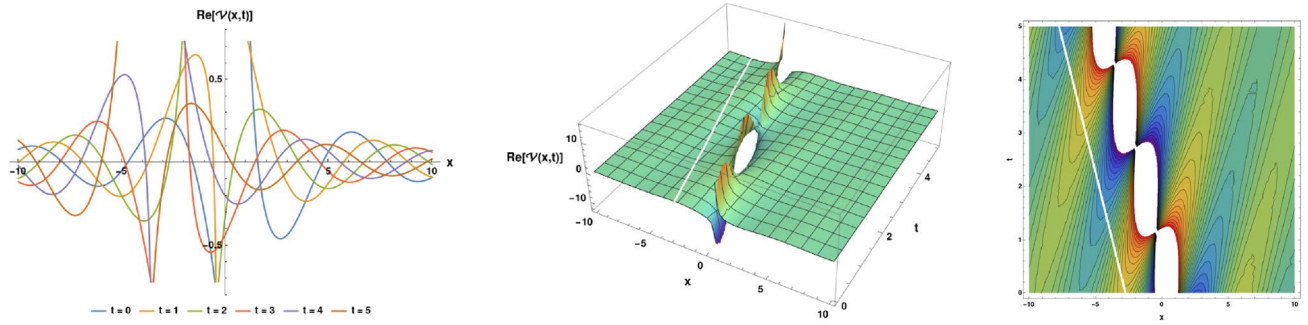

(a) 2D (b) 3D (c) Contour

Fig. 6 Graph of the real part of the solution $\mathcal{V}(x,t)$ corresponding to Eq. 6.6 for the following values of the constants, $k = \gamma = \mu = 1,\ \sigma = 0,\ \mathcal{A}_1 = 1,\ \mathcal{A}_2 = -1,\ \beta(t) = \sin(t)$ and $t = 0$ to 5

$|\mathcal{V}(x,t)|^2$. The choice of $|\mathcal{V}(x,t)|$ was motivated by its ability to clearly illustrate the amplitude, localization, and oscillatory features of the solutions. However, in many physical settings, particularly in optics, the observable intensity corresponds to $|\mathcal{V}(x,t)|^2$. We acknowledge this distinction and emphasize that $|\mathcal{V}(x,t)|$ was used here for clarity of visualization, while $|\mathcal{V}(x,t)|^2$ may be considered in practical contexts to represent measurable field intensity. In

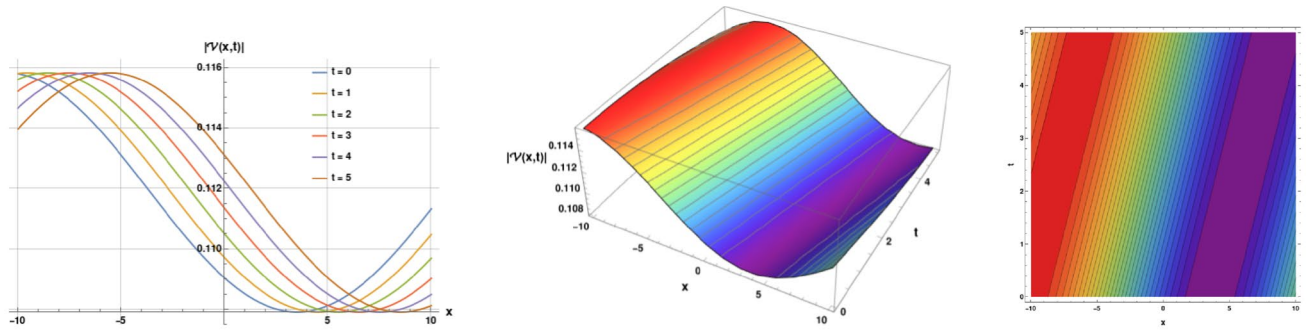

(a) 2D (b) 3D (c) Contour

Fig. 7 Graph of the solution $|\mathcal{V}(x,t)|$ corresponding to Eq. 6.7 for the following values of the constants, $k = \gamma = \mu = 1 = \rho = \eta,\ \sigma = 0,\ \lambda = 0.05\ \mathcal{A}_1 = 0.5,\ \mathcal{A}_2 = 0.5,\ \beta(t) = \sin(t)$ and $t = 0$ to 5

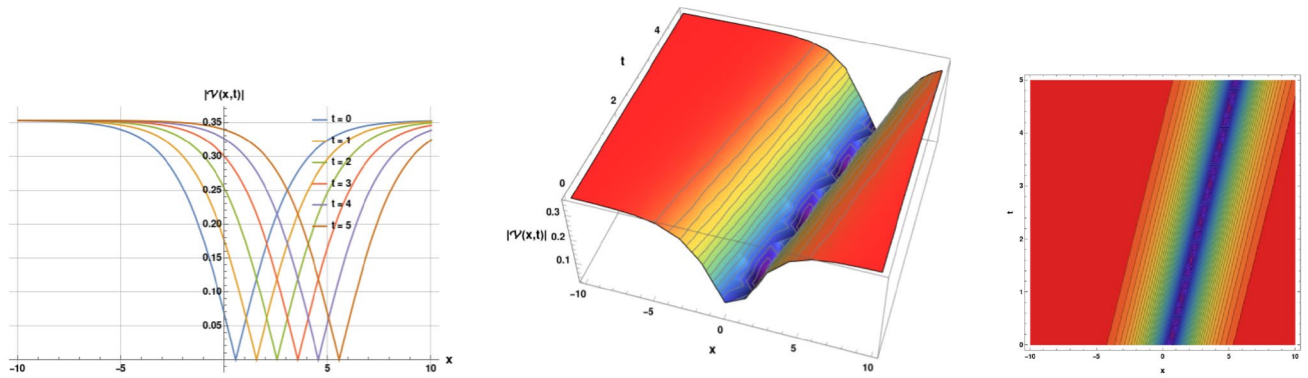

(a) 2D (b) 3D (c) Contour

Fig. 8 Graph of the solution $|\mathcal{V}(x,t)|$ corresponding to Eq. 6.8 for the following values of the constants, $k = \gamma = \mu = 1 = \rho = \eta,\ \sigma = 0,\ \lambda = -0.5\ \mathcal{A}_1 = -1,\ \mathcal{A}_2 = -1.5,\ \beta(t) = \sin(t)$ and $t = 0$ to 5

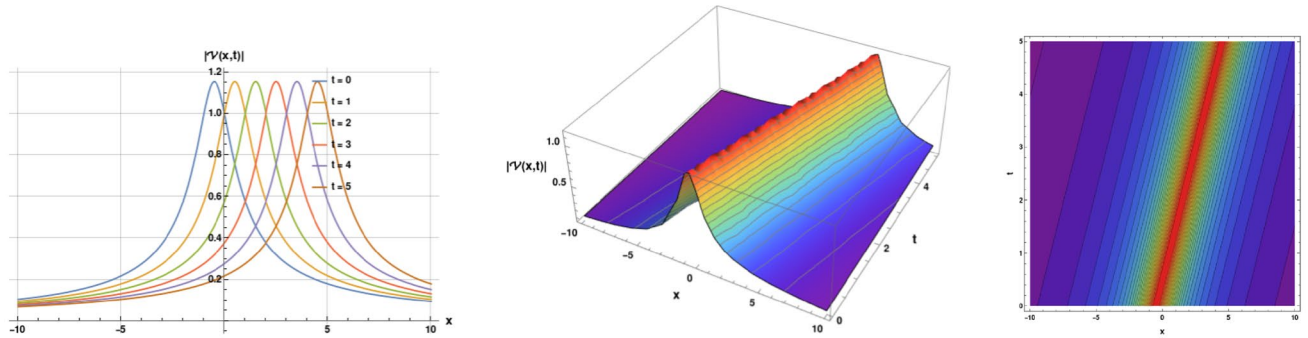

(a) 2D (b) 3D (c) Contour

Fig. 9 Graph of the solution $|\mathcal{V}(x,t)|$ corresponding to Eq. 6.9 for the following values of the constants, $k = \gamma = \mu = 1 = \rho = \eta,\ \sigma = 0,5\ \mathcal{A}_1 = 0.5,\ \mathcal{A}_2 = 0.5,\ \beta(t) = \sin(t)$ and $t = 0$ to 5

some figures, we have shown the real part $\mathfrak{R}(\mathcal{V}(x,t))$ of the solutions to highlight oscillatory waveforms more transparently, complementing the modulus-based plots. For the sake of simplicity and clarity, we have chosen nine representative solutions among the full set of obtained results to present graphically. To provide a clearer and more

comprehensive explanation, each solution is illustrated in three visual formats: 2D line plot, 3D surface plot, and contour plot. These graphical illustrations correspond to the solutions presented in Eqs. 6.1 to 6.9.

The corresponding graphs are shown in Figs. 1, 2, 3, 4, 5, 6, 7, 8 through 9, respectively. For each solution, subfigures (a), (b), and (c) represent the 2D, 3D, and contour plots, respectively. To maintain uniformity and reduce complexity, we have used the same domain $x \in [-10,\ 10]$ and time range $t \in [0,\ 5]$ for all plots. The values of the constants specific to each solution are provided in the respective figure captions. Although β (t) is theoretically linked to the temporal derivative of Brownian motion, we adopted simple deterministic functions (e.g., trigonometric) for illustrative purposes. This choice enables clear visualization of the solution structures, particularly their amplitude and oscillatory features. The analytical framework, however, remains valid for the general stochastic case. The values of the constants specific to each solution are provided in the respective figure captions. From Figs. 1 and 2, corresponding to Eqs. 6.1 and 6.2, it is evident that the solution profiles exhibit singular-periodic soliton behavior, characterized by repeating oscillatory patterns with localized intensity. Figure 3, based on Eq. 6.3, presents a kink-shaped wave, indicating a sharp traveling front. In contrast, the plot in Fig. 4 associated with Eq. 6.4 reveals a symmetric bell-shaped soliton. Figure 5, which visualizes Eq. 6.5, shows a highly localized singular soliton with a prominent peak. Figure 6, based on Eq. 6.6, demonstrates a rational rogue-wave-type solution that exhibits sharp localization in space-time. Figure 7, from Eq. 6.7, features a hybrid solution profile involving mixed trigonometric-hyperbolic characteristics. Meanwhile, Fig. 8, corresponding to Eq. 6.8, presents a dark soliton or anti-kink profile shaped by defocusing nonlinearity. Finally, Fig. 9, illustrating Eq. 6.9, shows a rational decaying solution, highlighting algebraic fall-off with singularity features.

These graphical interpretations provide both verification of the analytical results and qualitative insights into the diverse range of wave structures—solitonic, periodic, kink-type, rational, and rogue-wave-like—captured by the stochastic NLSEs under varying parameter regimes.

8 Conclusion

In this study, we have developed and applied the double-variable function expansion method to derive exact analytical solutions for three important forms of the stochastic nonlinear Schrödinger equation (NLSE): the focusing-type NLS^{+}, the defocusing-type NLS^{-}, and the NLSE with delta potential. By utilizing appropriate wave transformations, the stochastic partial differential equations were reduced to nonlinear ordinary differential equations, which were then solved through a structured expansion approach based on auxiliary functions. The solutions obtained span several distinct types: solitonic solutions, periodic oscillatory solutions, hyperbolic (localized solitary) solutions, and rational solutions, including rogue-wave-type profiles. These diverse solution structures capture the rich interplay between dispersion, nonlinearity, and stochastic effects, illustrating how multiplicative noise modulates wave amplitude, shape, and stability. Graphical interpretations further confirm the validity and richness of the analytical expressions, offering visual insights into their spatial–temporal behavior under different parametric conditions. The exact solutions serve as valuable references for validating numerical algorithms and enhancing the understanding of nonlinear wave dynamics in noisy environments. From a practical perspective, these findings hold relevance for fields, such as fiber optics, quantum communication, and nonlinear photonic systems, where wave stability and noise modulation are critical. The methodological framework presented here is robust and adaptable, and it may be extended in future work to higher-dimensional systems, coupled multi-component models, or those incorporating more complex stochastic perturbations such as colored noise or fractional operators.

Future research may extend the double-variable expansion method to higher-dimensional stochastic PDEs with more realistic perturbations such as colored or fractional noise, while its integration with numerical simulations and machine-learning-assisted solvers could further deepen insights into solution stability and accelerate the discovery of new wave structures in noisy physical systems.

Overall, this work contributes new analytical results on stochastic NLSEs and establishes the double-variable expansion method as a powerful tool for studying complex nonlinear wave phenomena.

Acknowledgements The author extends the appreciation to the Deanship of Postgraduate Studies and Scientific Research at Majmaah University for funding this research work through the project number (R-2025-2039).

Author Contributions Md Mamunur Rasid and K. El-Rashidy: conceptualization, methodology, investigation, writing—original draft preparation, and programming. Md Nur Hossain, O. H. Khalil, Wen-Xiu Ma, and Md Mamun Miah: programming, investigating, supervision, and writing—reviewing and editing.

Funding Not applicable.

Data Availability No datasets were generated or analyzed during the current study.

Declarations

Conflict of interest The authors declare that they have no conflict of interest.

Ethical approval I hereby declare that this manuscript is the result of my independent creation under the reviewers' comments. Except for the quoted contents, this manuscript does not contain any research achievements that have been published or written by other individuals or groups.

Conflict of interest The authors declare no conflict of interest.

References

Ahmad J, Aldwoah KA (2024) Stochastic wave solutions of fractional radhakrishnan-kundu-lakshmanan equation in optical fibers, Journal of Optics

Ahmed HK, Ali KK (2024) Optical solutions to the stochastic fokas–lenells equation with multiplicative white noise in itô sense using jacobi elliptic expansion function method, Optical and Quantum Electronics 56 (970)

Akbar MA, Akinyemi L, Yao S-W, Jhangeer A, Rezazadeh H, Khater MM, Ahmad H, Inc M (2021) Soliton solutions to the boussinesq equation through sine-gordon method and kudryashov method. Results Phys 25:104228

Al-Askar FM (2023) Optical solitary solutions for the stochastic sasa-satsuma equation, Results in Physics

Al-Askar FM (2025) Abundant optical solutions for the stochastic schrödinger–hirota equation in quantum mechanics, science and engineering, Modern Physics Letters B

Al-Essa LA, ur Rahman M (2024) Novel stochastic multi breather type, a-periodic, hybrid periodic and other type of waves of the schrödinger–hirota model, Optical and Quantum Electronics

Ali KK, Tarla S, Yusuf A (2023) Quantum-mechanical properties of long-lived optical pulses in the fourth-order kdv-type hierarchy nonlinear model, Optical and Quantum Electronics 55 (590)

Alkhidhr HA (2023) The new stochastic solutions for three models of non-linear schrödinger's equations in optical fiber communications via itô sense. Frontiers in Physics 11:1144704

Alraddadi I, Chowdhury MA, Abbas MS, El-Rashidy K (2024) Dynamical behaviors and abundant new soliton solutions via an efficient expansion method. Mathematics 12(13):2053

J.-I. S. and (2015) Final state problem for the cubic nonlinear schrödinger equation with repulsive delta potential, Communications in Partial Differential Equations 40 (2) 309–328

Ashraf F, Batool F (2024) Novel kink and multi wave soliton solutions to the stochastic phi-4 equation driven by the wiener process, Optical and Quantum Electronics

Atas SS, Ali KK, Sulaiman TA, Bulut H (2023) Dynamic behavior of optical solitons to the coupled-higgs equation through an efficient method. Int J Mod Phys B 37(15):2350144

Az-Zo'bi EA, Alomari QMM, Afef K et al (2024) Dynamics of generalized time-fractional viscous-capillarity compressible fluid model. Opt Quant Electron 56:629

Baskonus HM, Sulaiman TA, Bulut H, Aktürk T (2018) Investigations of dark, bright, combined dark-bright optical and other soliton solutions in the complex cubic nonlinear schrödinger equation with $\hat{I}$-potential. Superlattices Microstruct 115:19–29

Bhrawy A, Abdelkawy M, Biswas A (2014) Optical solitons in (1+1) and (2+1) dimensions. Optik 125(4):1537–1549

Butt AR, Umair M, Basendwah GA (2024) Exploring advanced nonlinear effects on highly dispersive optical solitons with multiplicative white noise, Optik

Cinar M, Secer A, Ozisik M, Bayram M (2022) Derivation of optical solitons of dimensionless fokas-lenells equation with perturbation term using sardar sub-equation method. Opt Quant Electron 54:1–13

Fukuizumi R, Ohta M, Ozawa T (2008) Nonlinear Schrödinger equation with a point defect. Annales de l'IHP Analyse non linéaire 25(5):837–845

Goodman RH, Holmes PJ, Weinstein MI (2004) Strong nls soliton–defect interactions. Physica D 192(3):215–248

Hamad IS, Ali KK (2024) Investigation of brownian motion in stochastic schrödinger wave equation using the modified generalized riccati equation mapping method, Optical and Quantum Electronics 56 (996)

Holmer J, Zworski M (2007) Slow soliton interaction with delta impurities. Journal of Modern Dynamics 1(4):689–718

Hossain MN, Miah MM, Alosaimi M, Alsharif F, Kanan M (2024) Exploring novel soliton solutions to the time-fractional coupled drinfel'd–Sokolov–Wilson equation in industrial engineering using two efficient techniques. Fract Fract 8:352

Hossain MN, El Rashidy K, Alsharif F, Kanan M, Ma W-X, Miah MM (2024) New optical soliton solutions to the biswas-milovic equations with power law and parabolic law nonlinearity using the sardar sub-equation method. Opt Quant Electron 56:1163

Hossain MN, Miah MM, Abbas MS, El-Rashidy K, Borhan JRM, Kanan M (2024) An analytical study of the mikhailov-novikov-wang equation with stability and modulation instability analysis in industrial engineering via multiple methods. Symmetry 16:879

Hossain MN, Rasid MM, Abouelfarag I, El-Rashidy K, Miah MM, Kanan M (2024) A new investigation of the extended sakovich equation for abundant soliton solution in industrial engineering via two efficient techniques. Open Physics 22(1):20240096

Hossain MN, Miah MM, Duraihem FZ, Rehman S, Ma W-X (2024) Chaotic behavior, bifurcations, sensitivity analysis, and novel optical soliton solutions to the hamiltonian amplitude equation in optical physics. Phys Scr 99:075231

Hossain MN, Alsharif F, Miah MM, Kanan M (2024) Abundant new optical soliton solutions to the biswas-milovic equation with sensitivity analysis for optimization. Mathematics 12:1585

Hossain MN, Miah MM, Hamid A, Osman GMS (2024) Discovering new abundant optical solutions for the resonant nonlinear schrödinger equation using an analytical technique. Opt Quant Electron 56:847

Hossain MN, Miah MM, Duraihem FZ, Rehman S (2024) Stability, modulation instability, and analytical study of the conformable time fractional westervelt equation and the wazwaz kaur boussinesq equation. Opt Quant Electron 56:847

Hossain MD, Boulaaras SM, Saeed AM, Gissy H, Hossain MN, Miah MM (2025) New investigation on soliton solutions of two nonlinear pdes in mathematical physics with a dynamical property: bifurcation analysis. Open Physics 23(1):20250155

Ismael HF, Younas U, Sulaiman TA, Nasreen N, Shah NA, Ali MR (2023) Non classical interaction aspects to a nonlinear physical model. Results in Physics 49:106520

Li Y, Geng X, Xue B, Li R (2021) Darboux transformation and exact solutions for a four-component fokas–lenells equation. Results in Physics 31:105027

Mimura M (1978) Backlund Transformation. Springer, Berlin, Germany

Mirzazadeh M, Sharif A, Hashemi MS, Akgü A (2023) Optical solitons with an extended (3+1)-dimensional nonlinear conformable schrödinger equation including cubic–quintic nonlinearity, Results in Physics 47

Newell A (1980) The inverse scattering transform. In: Bullough R, Caudrey P (eds) Solitons, vol 17. Topics in Current Physics. Springer, Berlin, Heidelberg, pp 142–183

Păuna A-M (2024) The auxiliary equation approach for solving reaction-diffusion equations. J Phys: Conf Ser 2719(1):012002

Paux J, Morin L, Gélébart L, Sanoko AMA (2025) A discrete sine–cosine based method for the elasticity of heterogeneous materials with arbitrary boundary conditions, Computer Methods in Applied Mechanics and Engineering 433, Part A 117488

Rasid MM, Miah MM, Ganie AH, Alshehri HM, Osman MS, Ma W-X (2023) Further advanced investigation of the complex hirota-dynamical model to extract soliton solutions, Modern Physics Letters B 1–18

Raza N, Seadawy AR, Arshed S, Khan KA (2024) Dynamical structure and variety of new fiber optical solitons of the stochastic ginzburg–landau model, Optical and Quantum Electronics

Rehman HU, Akber R, Wazwaz AM, Alshehri HM, Osman MS (2023) Analysis of brownian motion in stochastic schrödinger wave equation using sardar sub-equation method. Optik 289:171305

Rizvi STR, Mustafa B, Abbas SO (2024) Generation of optical dromions to generalized stochastic nonlinear schrödinger equation with kerr effect and higher order nonlinearity, Chinese Journal of Physics

Rizvi S, Seadawy AR, Younis M, Ali I, Althobaiti S, Mahmoud SF (2021) Soliton solutions, painlevé analysis and conservation laws for a nonlinear evolution equation. Results in Physics 23:103999

Shakeel M, Liu X, Abbas N (2025) Investigation of nonlinear dynamics in the stochastic nonlinear schrödinger equation with spatial noise intensity, Nonlinear Dynamics

Sulaiman TA, Younas U, Yusuf A, Younis M, Bilal M (2021) Shafqat-ur-rehman, extraction of new optical solitons and mi analysis to three coupled gross-pitaevskii system in the spinor bose-einstein condensate. Mod Phys Lett B 35(06):2150109

Wang P, Yin F, Rahman M, Khan M, Baleanu D (2024) Unveiling complexity: exploring chaos and solitons in modified nonlinear schrödinger equation. Results in Physics 56:107268

Younas U, Sulaiman TA, Yusuf A, Bilal M, Younis M, Rehman SU (2021) New solitons and other solutions in saturated ferromagnetic materials modeled by kraenkel-manna-merle system. Indian J Phys 96(1):181–191

Younas U, Sulaiman TA, Ren J (2022) Dynamics of optical pulses in dual-core optical fibers modelled by decoupled nonlinear schrödinger equation via gerf and neda techniques. Opt Quant Electron 54:738

Younas U, Sulaiman TA, Ren J, Yusuf A (2022) Lump interaction phenomena to the nonlinear ill-posed boussinesq dynamical wave equation. J Geom Phys 178:104586

Younas U, Sulaiman TA, Ren J (2023) Propagation of m-truncated optical pulses in nonlinear optics, Optical and Quantum ElectronicsIn press

Zafar A, Raheel M, Ali KK, Razzaq W (2020) On optical soliton solutions of new hamiltonian amplitude equation via jacobi elliptic functions, the. Eur Phys J Plus 135:1–17